MATHEMATICAL ANALYSIS OF PEDESTRIAN LOWER LEG IMPACTS

D.P. Wood and S. O Riordain
Wood & Associates,
Ireland

ABSTRACT

In this paper the impact loading and response of the pedestrian lower leg is examined using two models for the pedestrian. These are a two segment model with a frictionless pivot at the knee and a three segment model which has a second pivot at the hips. The models are used to examine the influence of bumper height on the kinematics of the lower leg and on the impulsive forces at both the impact point and at the knee joint. A model for the dynamic response of the lower leg and its angular rotation is included.

Comparison with the experimental cadaver responses reported by Cesari shows that the two segment model gives a high degree of correlation with the experimental results for lower leg rotation angle and peak impact force, while the three segment model does not. The tibia fracture/non-fracture prediction accuracy of both models is similar.

INTRODUCTION

There has been widespread research into pedestrian and car impact. One of the main areas of study has been pedestrian lower leg and knee injury. Aldman (1,2,3,4), Bacon (5), Pritz (6) and Eppinger and Pritz (7) and others have reported on experimental and analytical investigations. More recently Cesari (8) has detailed the results of a series of 20 cadaver tests of lower leg impact. Cesari reported on the influence of bumper height and impact speed on knee injury and on fracture of the lower leg. These tests also showed that lower leg impact results in a pivoting action at the knee.

The main purpose of this paper is to derive (a) a two segment model for the pedestrian which has a frictionless pivot at the knee and (b) a three segment model which has a second pivot at the hips and to compare the behaviour of both models with the cadaver results detailed by Cesari (8).

MATHEMATICAL MODELS

Detailed, complex multisegment pedestrian models have been developed by van Wijk et al (9) and MacLaughlin and Daniel (10) amongst others. van Wijk (9) has applied two, five, seven and fifteen segment models to the entire pedestrian and car collision process.

Specific mathematical models applied to leg impact by Aldman (2,3) and by Bacon (5) were based on the assumption that the lower and upper legs could be considered as a single rigid element with the hinge at the hip. Aldman (2) also used a mechanical model for the leg which included a mechanical model of the knee joint.

The models examined here for lower leg impact are a two segment model with a frictionless hinge at the knee and a three segment model with a second hinge at the hips. In the two segment model the lower segment represents both legs while the upper segment represents the rest of the body. In the three segment model both thighs are represented by a separate segment.

The analysis is based on the derivation of the impulsive forces which result from lower leg impact. The force deflection or compliance characteristics of the bumper and leg do not have to be considered when using this approach. Wood (11) has shown that this method can be applied to pedestrian impact. The body geometry and mass data used are based on Gibson (12). The body geometry is expressed as the ratio of 'l' which is half of the lower leg height (ie knee height=2xl). The masses are expressed as the ratio of the mass of both legs. The models and data are detailed in figure 1.

The calculated impulsive forces are expressed in non-dimensional form as ratios of $M_l.V_{cf}$ where V_{cf} is the post- impact velocity at the bumper contact point. These non-dimensional ratios can also be considered as the "equivalent mass ratios" with respect to the mass of the lower legs. The non-dimensional impulsive forces due to the bumper impact are I_b bumper impulse, I_{kh} knee horizontal shear impulse and I_{kv} knee vertical impulse. The vertical knee impulse I_{kv}, is derived using the model for the knee given by Aldman (2).

Hence

$$I_{kv} = BM_{ok} / c \qquad (1)$$

where BM_{ok} is the non-dimensional bending moment impulse at the knee and c is the condyle width.

EFFECT OF GROUND TO FOOT FRICTION

A friction impulse is developed between the foot and the ground. This impulse will resist movement by the foot and consequently will act in the opposite direction to that of the motion of the foot. The magnitude of the friction impulse will depend on the time duration of the impulse between the bumper and lower leg.

$$I_f = \mu.g.(M_t).\Delta t \qquad (2)$$

where Δt is the duration of the impulse, and μ the coefficient of friction between the ground and the feet. Under normal conditions the coefficient of friction between the foot and the ground is in the range 0.3 to 0.6. For convenience of manipulation of the equations the ratio of the friction impulse to the leg impulse $I_f/M_l.V_l = \alpha$ is used.

LOWER LEG INJURY CRITERIA

Fractures of the tibia or fibula can occur as can fracture or dislocation injuries to the knee or ankle joint. Also ligament injuries of the knee or ankle can occur. Knee injuries are of particular concern as long term disability can result. Hull and Allen (13) and Asang (14) indicate that tibia fracture in flexion is related to the bending moment exerted on the leg. The mean bending moment for tibia fracture is 225 Nm with minimum and maximum values of 150 Nm and 300 Nm respectively.

Aldman (2) indicates that knee injury can occur during the impact to the lower leg and also during the subsequent motion of the lower leg relative to the thigh. Eppinger (7) details an acceleration criterion to minimise knee injury during impact. Cesari (8) shows that knee injury is related to the angle of rotation of the lower leg relative to the thigh. This relative rotation is resisted by the knee ligaments.

The dynamic motion of the lower leg relative to the thigh can be modelled by representing the lower leg and knee as a spring/mass system where the knee acts as a torsion spring, refer figure 2. Provided the impulse duration is short by comparison with that of the lower leg/knee spring mass system, it can be shown that the angular response of the lower leg to an impulse is

$$\theta_{max} = W_{rel} \cdot (M_l \cdot (K_l^2 + l^2)/S)^{1/2} \qquad (3)$$

where θ_{max} is the maximum distortion angle between the lower leg and the thigh, K_l radius of gyration of lower leg, l half leg height and S the spring rate of the knee joint. W_{rel} is the angular velocity of the lower leg relative to the thigh. Gibson (12) indicates that the spring rate of the knee is in the order of 1700 Nm/Radian. For a leg mass of 4.4 kg this model indicates that the time for the lower leg to flex to the maximum angle and return to the undeflected position is of the order of 47 ms.

KINEMATICS OF LOWER LEG IMPACT

Examination of the two and three segment models shows that the kinematics of the lower leg and thigh are similar for both models. In the three segment model the translational and rotational movements of the upper body are in the opposite directions to those of the thigh.

Analysis of the models indicates that the kinematics can be divided into five distinct regions depending on the height of the bumper. The transition between each region is characterised by a specific contact height which is a function of the pedestrian geometry and mass and of the friction impulse. In the three segment model the transitions occur at lower impact heights than for the two segment model. Figure 3 shows the kinematic behaviour for the two segment model. The equations for the transition points are detailed in appendix 1.

Region 1 This is for low bumper levels close to the foot and ankle. Here the foot moves forward and upward while the knee moves backwards towards the car. The transition to region 2 occurs when the upper segment remains upright and stationary (at 29% of knee height, μ=0). There is no horizontal impulse at the knee. This point is a function only of leg geometry and the friction impulse ratio.

Region 2 Here both lower leg and thigh rotate in the same direction, the foot outwards and upwards and the hips backwards towards the car, however the rotational velocity of the lower leg is higher than the upper (thigh) segment. The transition to region 3 occurs when the rotational velocities of the lower leg and thigh are the same. This occurs at 53% of knee height (3 segment model, μ=0) and 69 % of knee height (2 segment, μ=0). At this point there is no relative rotation between the lower leg and thigh as a consequence of the impact.

Region 3 In this region the lower leg continues to rotate forward bringing the foot upwards. However the rate of rotation is slower than that of the thighs and rotation of the lower leg ceases at the transition to region 4. At this point, 65% of knee height (3 segment, μ=0), 77% of knee height (2 segment, μ=0), the impact ceases to cause the lower leg to rotate, the leg slides forward while remaining upright.

Region 4 Here the leg and thigh rotate in opposite directions. The foot rotates backwards relative to the centre of gravity of the lower leg and curls under the bumper. As the contact point moves higher the velocity of rotation of the lower leg continues to increase until the translational velocity of the foot due to lower leg rotation counterbalances the forward velocity of the lower leg and the foot remains stationary and the ground friction has no effect.

For bumper heights below this level the friction impulse opposes forward motion of the lower leg and increases the impulsive force transmitted by the bumper to the lower leg. Above this contact height the foot has a tendancy to move backwards along the ground relative to its position before impact. Consequently the friction impulse which acts to oppose this foot motion acts in the same direction as the bumper impulse reducing its magnitude. There is a range of leg contact positions to each side of the "no friction" point for which there is also no movement of the foot. Over this range the value of the friction impulse is less than the maximum value determined from the coefficient of friction.

Region 5 Contact points above 91% (2 segment, μ=0). Here the velocity of the foot is backwards towards the car. The transitions between the regions are summarised for μ=0 as follows

Transition point	Percent of Knee Height	
	2 Segment	3 Segment
Thigh+upper body remain upright and stationary	29%	29%
No relative rotation between lower leg and thigh	69%	53%
Lower leg remains upright and slides forward	77%	65%
Foot remains stationary on ground	91%	85%

Table 1. Lower leg kinematics

The effect of the friction impulse is to reduce the contact heights at which the transition points occur. The extent of the reduction depends on the magnitude of the friction impulse. This effect is shown in figure 4 for the two segment model. For high friction impulses there is an extended range of contact positions, close to the knee where the foot remains stationary on the ground.

The three segment model shows that in the presence of friction the contact height for no relative rotation between lower leg and thigh will be less than 53% of knee height. By comparison the two segment model gives values below 69%. These values compare with 56% obtained by Aldman (2) in tests with a mechanical model and 65% by Cesari (8) in cadaver tests.

EFFECT OF IMPACT LOCATION ON IMPULSIVE FORCES

Figure 5 shows the variation in the impulsive force at the contact point, I_b when μ=0. The peak value occurs at 65% of knee height (3 segment model) and at 75% of knee height (2 segment). For both models the value of I_b is less than 1 at contact points below 40% of knee height (i.e. the equivalent mass of the pedestrian is less than the leg mass).

Figure 5 shows the variation in the maximum bending moment impulse "B_{mo}". For low contact points the maximum bending moment is positive (corresponding to tensile bending stresses in the side of the leg facing the bumper). The maximum bending moment occurs above the midpoint of the lower leg. At 24% of knee height the maximum positive and negative bending moments are the same. There are two locations of maximum bending moment, at the contact point and above the midpoint of the lower leg. Above this point the maximum bending moment is negative and occurs at the contact point. The magnitude of the maximum bending moment varies with contact height as seen in figure 5. The peak value of the maximum bending moment occurs at 64% of knee height (3 segment model) and 70% of knee height (2 segment model).

Figure 5 shows the ratio of the normalised bending moment impulse to the bumper impulse. The ratio is a maximum at 65% of knee height and reduces to less than 1/3 of the peak value for impacts at knee level. This indicates that the forces required for tibia fracture will be three times higher when the contact point is at the knee compared with a contact point of 65% of knee height.

Figure 6 shows the variation in the impulsive forces transferred through the knee during impact. The peak knee impulse occurs at 83% of knee height (3 segment model) and 86% of knee height (2 segment model).

The relative lower leg to thigh rotational velocities for the two and three segment models are shown in figure 6. The three segment model predicts higher relative velocities for contact points close to the knee and the contact point for zero relative velocity is lower.

COMPARISON WITH CADAVER TESTS

Cesari (8) published the results of 20 cadaver tests. In 11 of the 20 tests the impact was to the lower leg. The results published included lower leg to thigh angle and peak force on the right leg. The force pulse on the right leg had a duration of 0.028 seconds. The model for lower leg/thigh angle was combined with the 2 and 3 segment impact models to calculate the maximum angle of rotation. Figure 7 and 8 compare the calculated lower leg/thigh angles with the experimental results. This comparison shows that the 3 segment model gives a much lower leg contact point for zero angle than obtained experimentally. The 2 segment calculations match the experimental data more closely. Regression analysis of the absolute values of the calculated and experimental angles shows

Model	Equation	r	Significance
2 Segment	$\lvert\theta_{act}\rvert = 4.220 + 1.026\,\lvert\theta_{calc}\rvert$ (deg)	0.888	$p<0.5\%$
3 Segment	$\lvert\theta_{act}\rvert = 2.875 + 0.560\,\lvert\theta_{calc}\rvert$ (deg)	0.619	$p>5.0\%$

Table 2. Comparison of experimental and calculated lower leg/thigh angle

Eppinger (7) indicates that the force impulse to the lower leg takes a sinusoidal form. Figure 9 and 10 compare the calculated peak forces, based on a sine pulse shape with the experimental results. Regression analysis shows

Model	Equation	r	Significance
2 Segment	$F_{act} = -780 + 1.068\,F_{calc}$ (N)	0.8717	$p<1\%$
3 Segment	$F_{act} = 714 + 1.028\,F_{calc}$ (N)	0.6806	$p<5\%$

Table 3. Calculated and Experimental peak forces

Cesari (8) also reported on the incidence of fractures (AIS 2+) to the long bones of the lower leg. Table 4 compares the calculated prediction of tibia fracture based on a minimum bending moment of 150 Nm (13,14) with Cesari's results.

Impact Speed kph	%Knee height	2 Segment Model	Cesari Results	3 Segment Model
	60	Y*	N	Y*
20	75	Y	Y	Y
	90	N	N	N
	60	Y	Y	Y
32	75	Y	Y	Y
	90	Y*	N	N
	60	Y	Y	Y
39	75	Y	Y	Y
	90	Y	Y	N*

Table 4. Calculated and Experimental Long Bone Injury

Note : * indicates where prediction differs from Cesari's results.

The two segment model calculates tibia fractures in 2 cases where Cesari found no AIS 2 long bone injury. The three segment model calculates tibia fracture in one case where there was no injury and predicts no tibia fracture in a second case where an AIS 2 long bone injury occurred.

DISCUSSION

Comparison of the two and three segment models with the test results from Cesari (8) shows that there is a high degree of correlation between the two segment model and the experimental results in respect of the maximum lower leg to thigh angle and of peak impact force at the contact point. The three segment model gives a poor correlation with the experimental results for these parameters. In the models used the effect of including the third segment (pivot at hip) is to reduce the effective mass of the upper body reflected onto the lower legs. This is the reason why the results from the three segment model are different from the two segment model. However both models predict a similar pattern of kinematic behaviour with contact height.

Modelling of a pivoting action at the hip is included in complex multisegment models, refer van Wijk (9) and Huijbers (15). van Wijk (9) only includes the hip pivot in 5 segment and more complex models. He has shown (9) that a two segment model with a pivot at the knee can be applied to the entire pedestrian-car collision with a high measure of agreement between predicted and test results. The analysis in this paper shows that a two segment model with a pivot at the knee can be used to represent lower leg impacts.

The bending moment criterion from Hull (13) and Asang (14) was used in conjunction with the calculated peak force for a sinusoidal pulse to predict tibia fracture. Comparison with Cesari's (8) results for long bone, AIS 2 injury shows that both the two and three segment models predicted fracture/no fracture correctly in 7 out of 9 cases. In the remaining 2 cases the two segment model predicted fracture when there was no AIS 2 injury. The three segment model predicted no fracture in one case when there was an AIS 2 long bone injury. In the other instances a fracture was predicted when none occurred, refer table 4.

The models shows that force necessary to cause tibia fracture varies significantly with impact contact height. Some preliminary investigations using the two segment model indicates for moderate and high foot friction impacts that tibia fracture could occur for impact forces in the region of 1300 N.

Aldman (1,2,3) indicated that the horizontal knee shear force had a minimum between the mid-tibia and the foot and a maximum at about 78% of knee height. The two segment model gives a maximum knee shear force at 86% of knee height when $\mu=0$. The location of this maximum will decrease with increasing foot to ground friction. Aldman (2) obtained no relative lower leg to thigh rotation for a contact height of 56% of knee height. Cesari (8) obtained 65% of knee height for no relative rotation. In the absence of foot to ground friction the two segment model predicts no relative rotation at 69% of knee height. The model shows for the conditions pertaining in Cesari's tests that the relative leg/thigh rotation is zero between 61% and 65% of knee height.

Examination of the kinematics of lower leg impact shows that for impact points above 77% of knee height (2 segment model) the rotation of the lower leg is backwards and the lower portion of the leg and foot rotates under the bumper. The foot to ground friction is shown to lower the contact height at which rotation under the bumper occurs. This effect is particularly pronounced at low speed and for long impulse durations.

Both two and three segment models indicate that the equivalent mass of the pedestrian is greater than the mass of the legs for contact points above 40% of knee height. Bacon (5) reported similar findings from dummy tests. Eppinger (7) and Cesari (8) however report equivalent masses less than the static leg mass of the 50%ile male.

The approach used here of determining the impulsive forces seperately from the dynamics of the impact process allows the kinematics and impulsive forces to be examined analytically. This approach is facilitated by use of a small number of segments and gives insights into the general mechanisms of pedestrian lower leg impact and parameter sensitivity. Such an approach is complementary to the complex detailed modelling necessary for exact detailed replication of the impact process.

REFERENCES

1. Aldman, B. et al "Physical simulation of human leg-bumper impacts" Proc 1979 IRCOBI Conf p232-242.

2. Aldman, B. et al "An experimental model for the study of lower leg and knee injuries in car-pedestrian accidents" Proc 1980 IRCOBI Conf p180-193.

3. Aldman, B. et al "An experimental model for the study of lower leg and knee injuries in car pedestrian accidents" Proc 1980 ESV Conf p841-848.

4. Aldman, B. et al "Experimental study of a compliant bumper system" Proc 27th Stapp car crash Conf 1983 P-134 p287-297 (SAE 831623)

5. Bacon, D. and Wilson, M. "Bumper characteristics for improved pedestrian safety" Proc 20th Stapp car crash Conf 1976 p391-429 (SAE 760812).

6. Pritz, H. et al "Body : vehicle interaction : experimental study" Final technical report of contract no DOT-HS-361-3-745 Report no. DOT-HS-801-474, 1975.

7. Eppinger R. and Pritz H. "Development of a simplified vehicle performance requirement for pedestrian injury mitigation" Proc 7th ESV Conf 1979 p713-724.

8. Cesari, D. et al "Interaction between human leg and car bumper in pedestrian tests" Proc 1988 IRCOBI Conf p259-269.

9. van Wijk, J., et al "MADYMO pedestrian simulations" Proc SAE Symposium on Pedestrian impact, injury and assessment, 1983, P-121, paper 830060, p109-117.

10. Mac Laughlin, T.G. and Daniel, S. "A parametric study of pedestrian injury" Office of crashworthiness, NHTSA, USA.

11. Wood D.P. "Application of a rigid body impact model to the pedestrian-car collision" Proc 1988 IRCOBI Conf p241-252.

12. Gibson, T. et al "Pedestrian head impacts : development and validation of a mathematical model" Proc 1986 IRCOBI Conf p165-176.

13. Hull, M.L., and Allen, K.W., "Design of an actively controlled snow ski release binding" J.Biomechanical Eng., Trans. ASME Vol.103, Aug.1981 p138-145.

14. Asang, E. "20 Jahre Skitraumatologie" Technical University of Munich, 1970.

15. Huijbers, J. et al "Experimental and mathematical car-bicycle collision simulations" SAE 881726 p197-211.

APPENDIX

EQUATIONS FOR TWO SEGMENT MODEL

m_t = Total mass of body

m_c = Mass of car

m_b' $= m_b \cdot K_b^2/(K_b^2 + h^2)$

V_{ci} = Velocity of car before impact

V_{cf} = Velocity of car after impact

$\ell\omega_t/V_{ci}, \ell\omega_b/V_{ci}$ = Normalised rotational velocities

$V_t/V_{ci}, V_b/V_{ci}$ = Normalised velocities

I_{kh} = Horizontal knee impulse due to bumper impact

$= m_b V_b / m_t V_{cf}$

I_{kv} = Vertical knee impulse due to bumper impact

$= BM_{ok}/c$

I_{kt} = Total knee impulse $= (I_{kh}^2 + I_{kv}^2)^{1/2}$

I_f = Friction impulse

$= \mu . m_t . g . \Delta t$

Δt = Duration of bumper impulse

α $= I_f / m_t V_t$

I_b = Impulse at contact point on bumper

$= (m_t V_t (1 + \alpha \, \mathrm{Sign}(V_t + \ell\omega_t)) + m_b V_b)/m_t V_{cf}$

B_{mo} = Normalised bending moment impulse

$= B.M.\Delta t / m_t . \ell . V_{cf}$

BM_{ok} = Normalised bending moment at knee

$$\ell\omega_t/V_t = \ell\left\{\frac{m_t(\ell-b) + m_b'(2\ell-b) - \alpha\, m_t . b\, \mathrm{Sign}(V_t + \omega_t \ell)}{m_t . K_t^2 + m_b' . \ell . (2\ell - b)}\right\}$$

$$V_b/V_t = (m_b'/m_b)(1 - \ell\omega_t/V_t) \quad ; \quad \ell\omega_b/V_t = h/K_b^2 . V_b/V_t \quad ; \quad V_{cf}/V_t = 1 + (1 - b/\ell)\ell\omega_t/V_t$$

$$V_t/V_{ci} = \frac{m_c(m_t K_t^2 + m_b' \ell(2\ell - b))}{(m_c + m_b + m_t(1 + \alpha\,\mathrm{Sign}(V_t + \ell\omega_t))).(m_t K_t^2 + m_b' \ell(2\ell-b)) - (m_b'\ell + m_c(b-\ell))(m_t(\ell-b) + m_b'(2\ell-b) - \alpha m_t b\,\mathrm{Sign}(V_t + \ell\omega_t))}$$

Bending Moments

between 0 and b

$$B.M.\Delta t = -I_f a\,\mathrm{Sign}(V_t + \omega_t \ell) - (m_t/2\ell)(V_t a^2/2 + \omega_t \ell a^2/2(1 - a/3\ell))$$

from b to 2ℓ

$$B.M.\Delta t = -I_f a\,\mathrm{Sign}(V_t + \omega_t \ell) - (m_t/2\ell)(V_t a^2/2 + \omega_t \ell a^2/2(1 - a/3\ell)) + I_b(a - b)$$

where a is distance from ground to point at which B.M. is calculated

KINEMATIC TRANSITION EQUATIONS

$$(b/\ell)_{\omega_b = 0} = \frac{1 - K_t^2/\ell^2}{1 + \alpha}$$

$$(b/\ell)_{\omega_t = \omega_b} = \frac{1 + (K_b^2/(K_b^2 + h^2))(2m_b/m_t + h\ell/K_b^2(1 - K_t^2/\ell^2))}{1 + \alpha + (K_b^2/(K_b^2 + h^2))(1 + \alpha + m_b/m_t)}$$

$$(b/\ell)_{\omega_t = 0} = \frac{1 + 2m_b'/m_t}{1 + m_b'/m_t + \alpha}$$

$$(b/\ell)_{NFM} = \frac{1 + 4m_b'/m_t + K_t^2/\ell^2}{1 + 2m_b'/m_t \pm \alpha} \qquad \text{no foot movement}$$

for Three Segment Model substitute m_b'' in equations for m_b' where

$$m_b'' = \frac{m_t(K_t^2(m_t + m_b') + (t - t_c)^2 m_b')}{m_t(K_t^2 + t_c^2) + m_b' t^2} \quad , \quad \text{also}$$

$$(b/\ell)_{\omega_t = \omega_b} = \frac{(1 + 2m_b'')(m_t K_t^2 + m_b' t^2 + m_t t_c^2) + (1 - K_t^2)(m_b' . t . \ell + m_t . t_c . \ell)}{(1 + \alpha + m_b'')(m_t K_t^2 + m_b' t^2 + m_t t_c^2) + (m_b' . t . \ell + m_t t_c \ell)(1 + \alpha)}$$

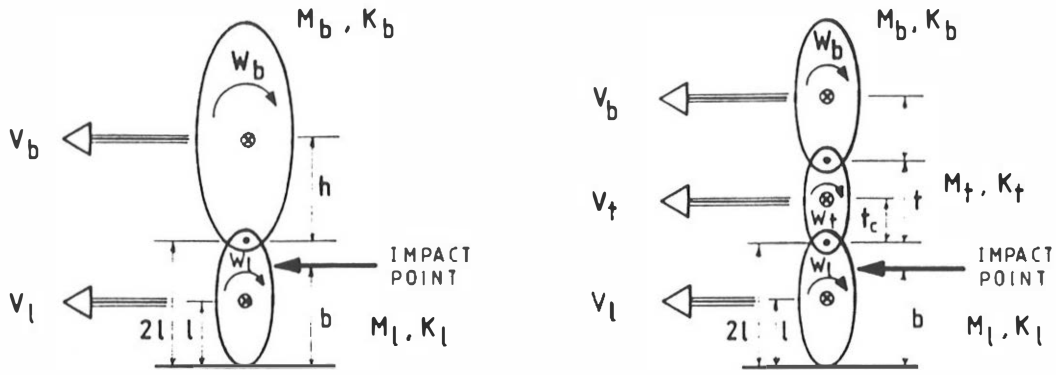

2 SEGMENT MODEL

3 SEGMENT MODEL

ITEM	2 SEGMENT MODEL	3 SEGMENT MODEL
K_l / L	0·656	0·656
K_t / L	——	0·472
K_b / L	1·066	0·892
T / L	——	1·691
T_c / L	——	0·964
H / L	2·467	1·332
M_t / M_l	——	1·733
M_b / M_l	7·33	5·600
$M_b^{\prime} / M_l$	1·15	0·421

FIGURE 1 MODELS

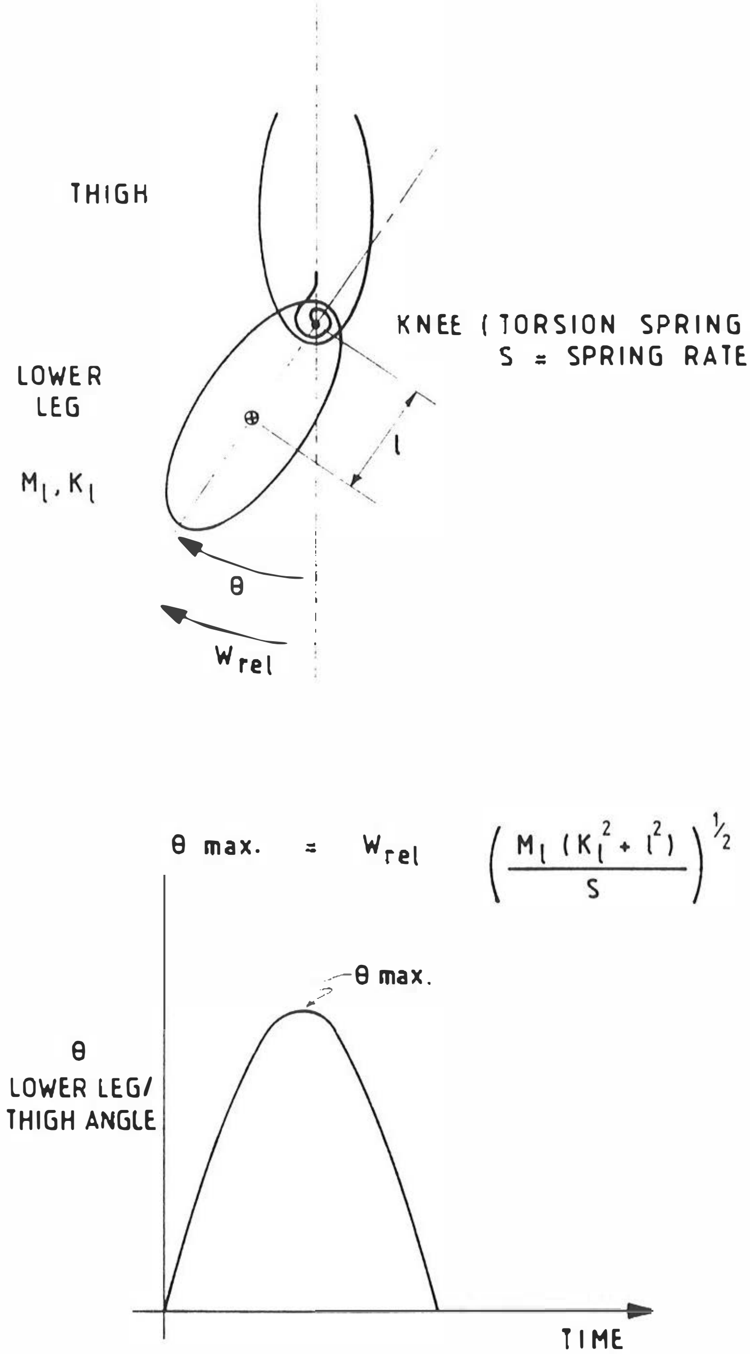

FIG.2. MODEL of DYNAMIC RESPONSE of LOWER LEG

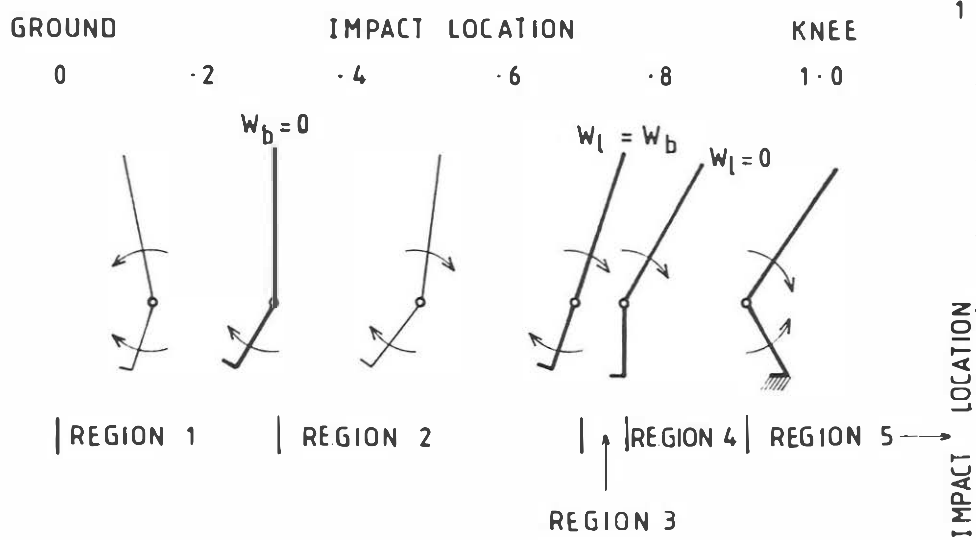

FIG. 3. KINEMATICS of LOWER LEG IMPACT for 2 SEGMENT MODEL

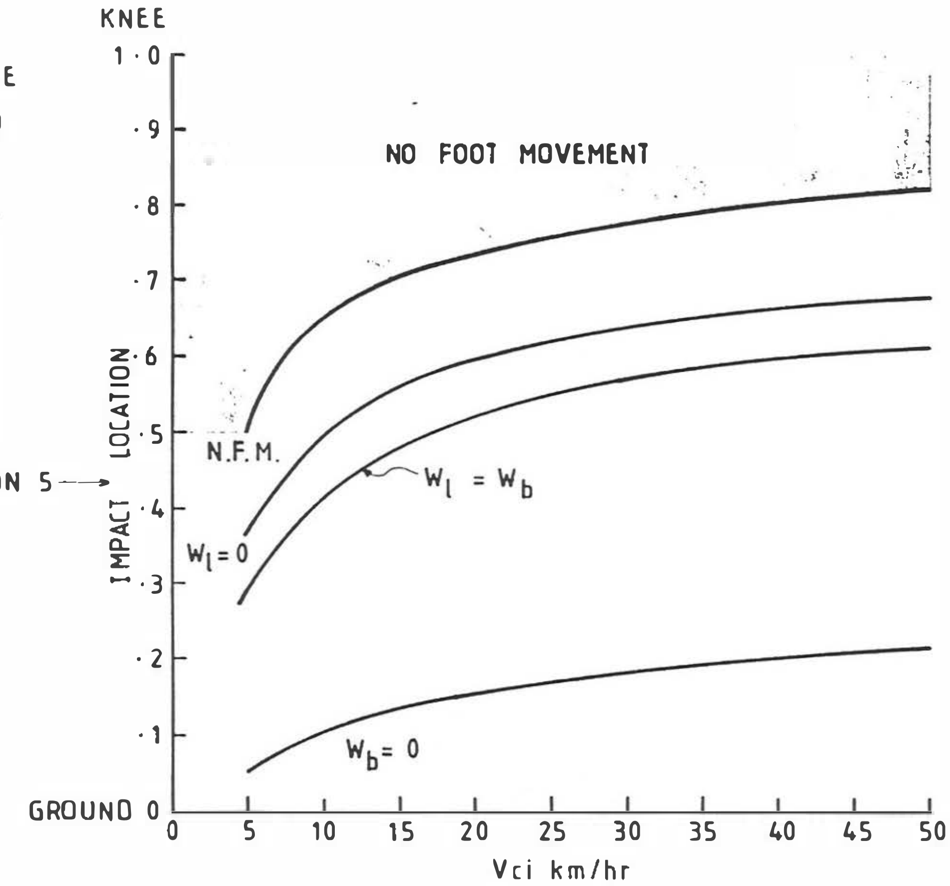

FIG. 4. EFFECT of FRICTION IMPULSE on KINEMATICS (GRAPH for $\mu = 0·5$ and ΔT ·06 sec.)

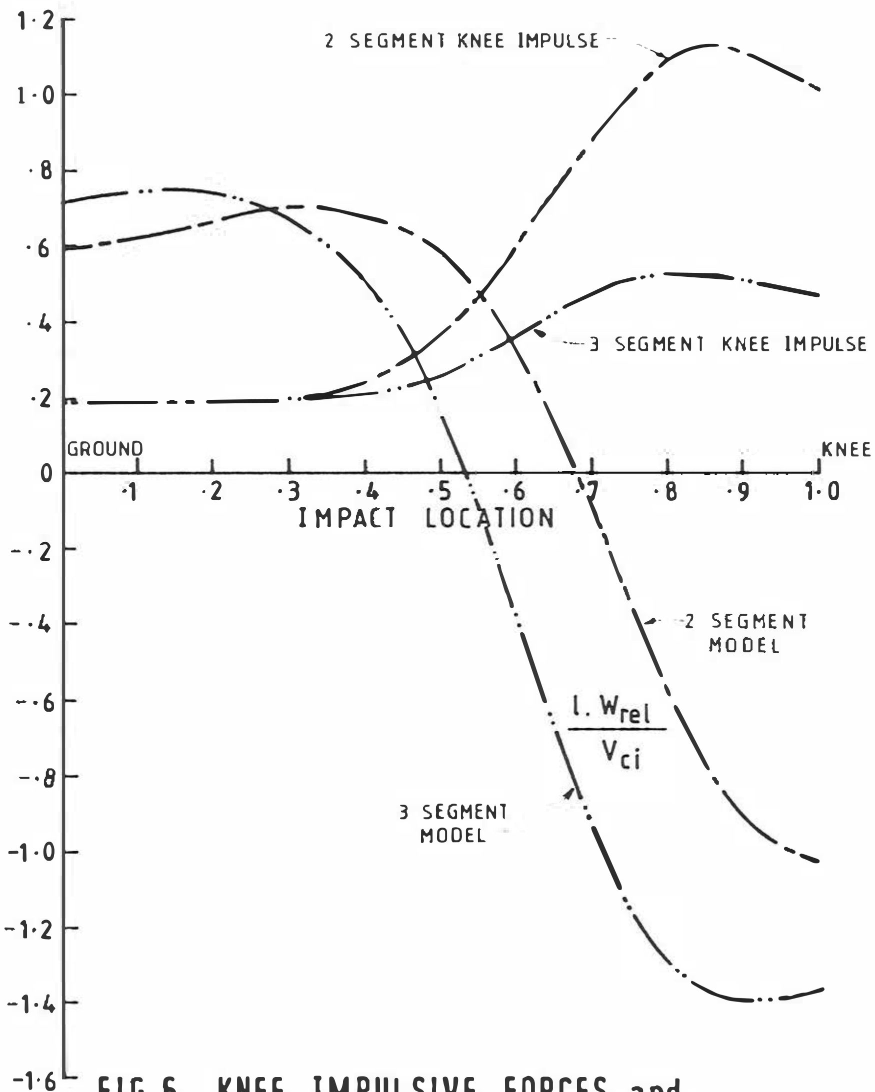

FIG. 6. KNEE IMPULSIVE FORCES and LEG/THIGH ROTATION

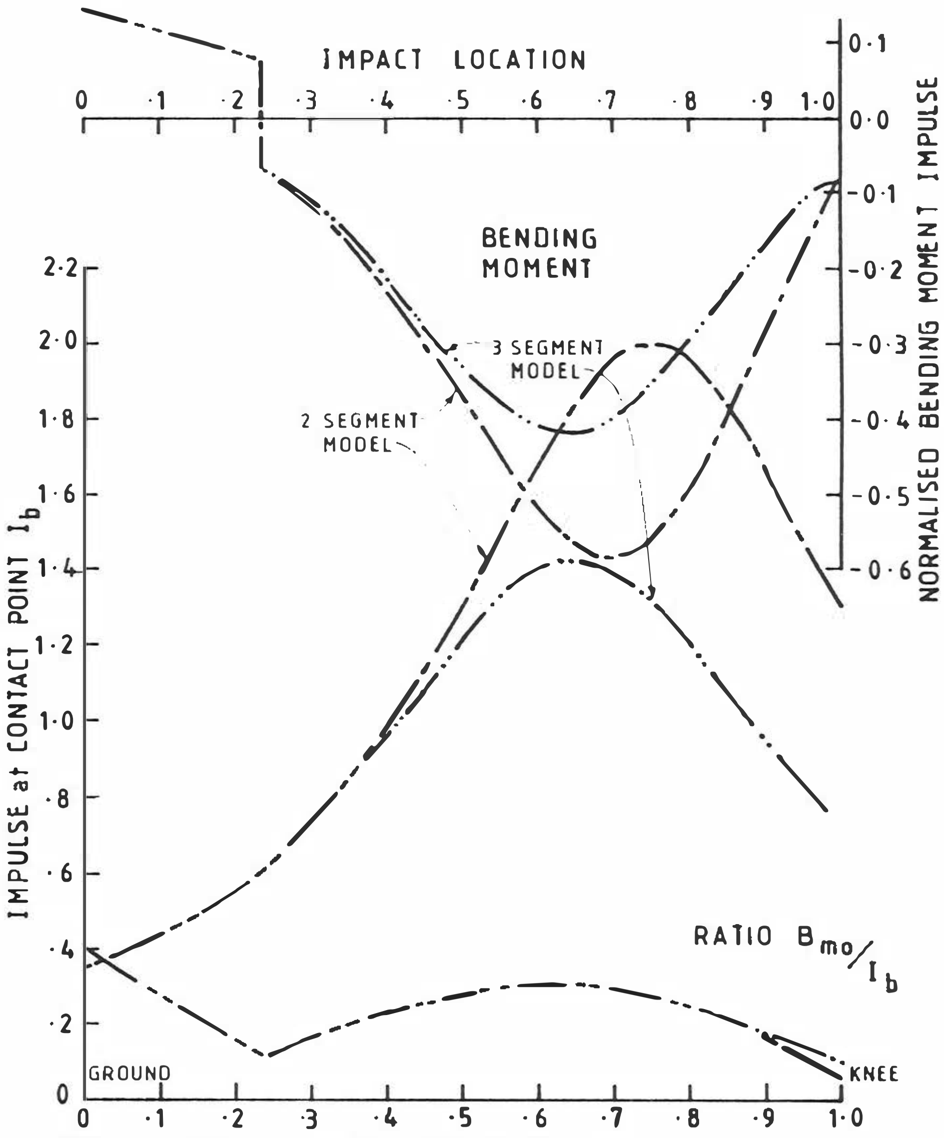

FIG.5. IMPULSE at CONTACT POINT and MAXIMUM BENDING MOMENTS

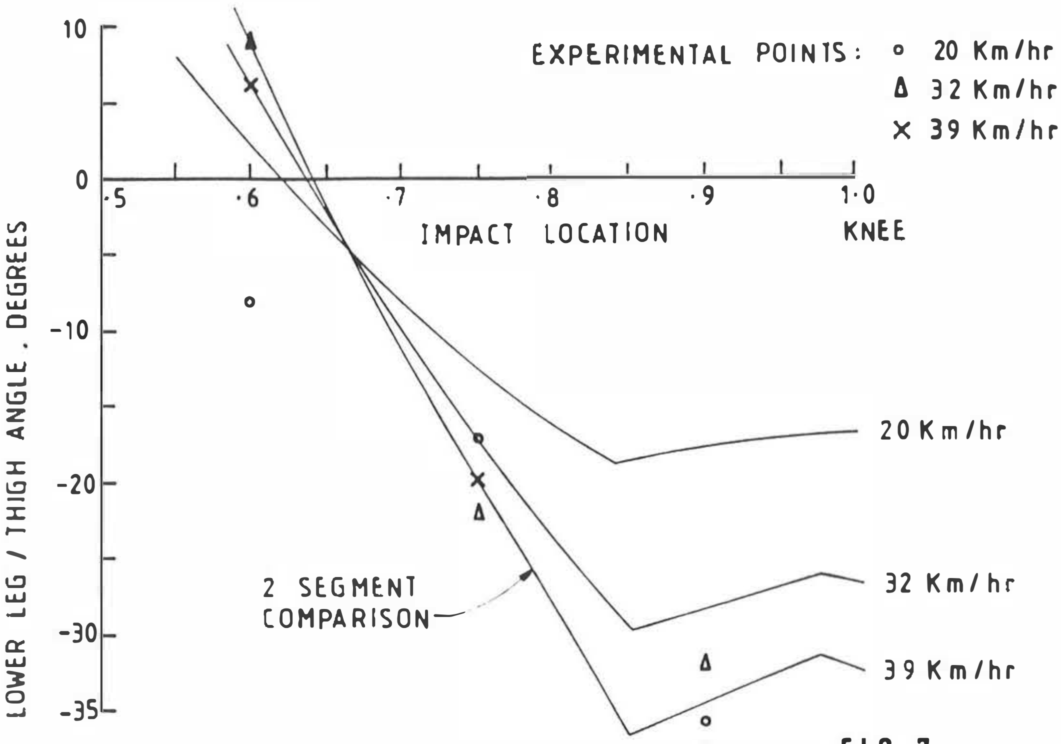

FIG. 7.

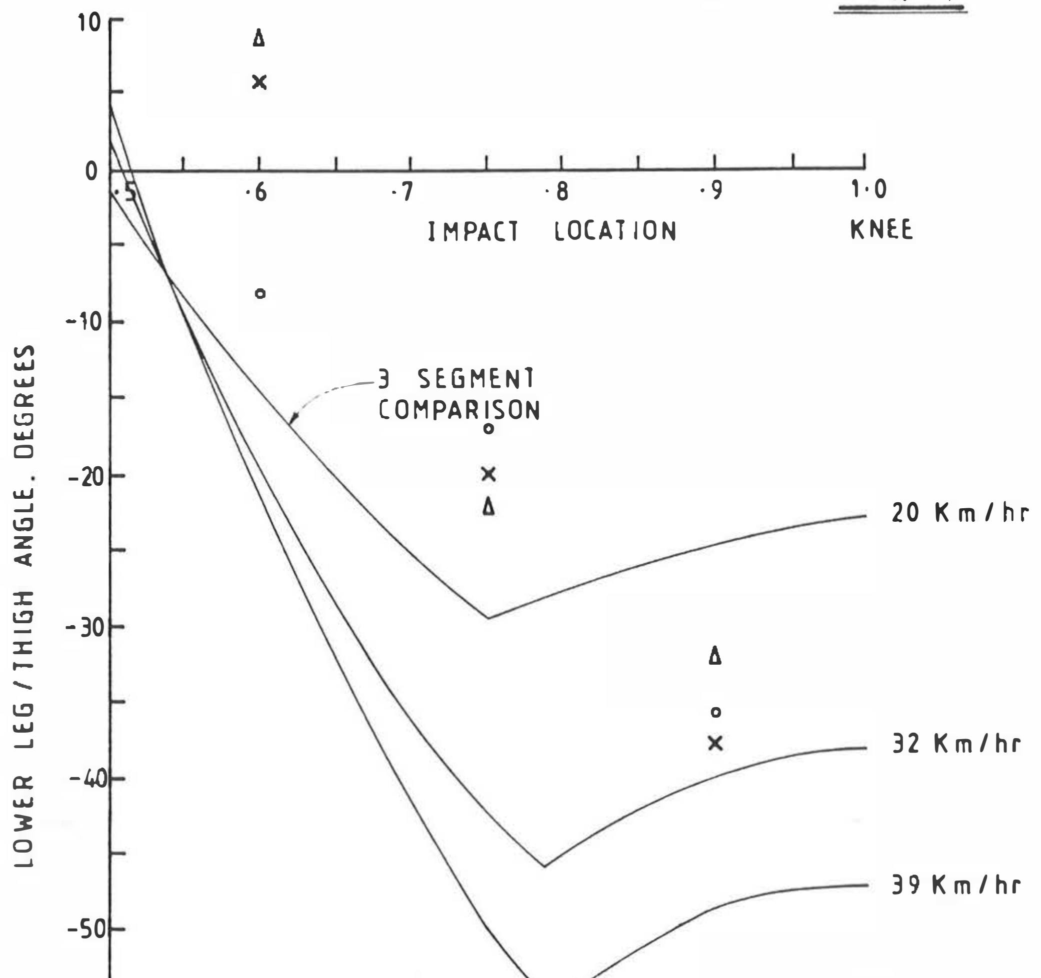

FIG. 8.

MAXIMUM LOWER LEG / THIGH ANGLE

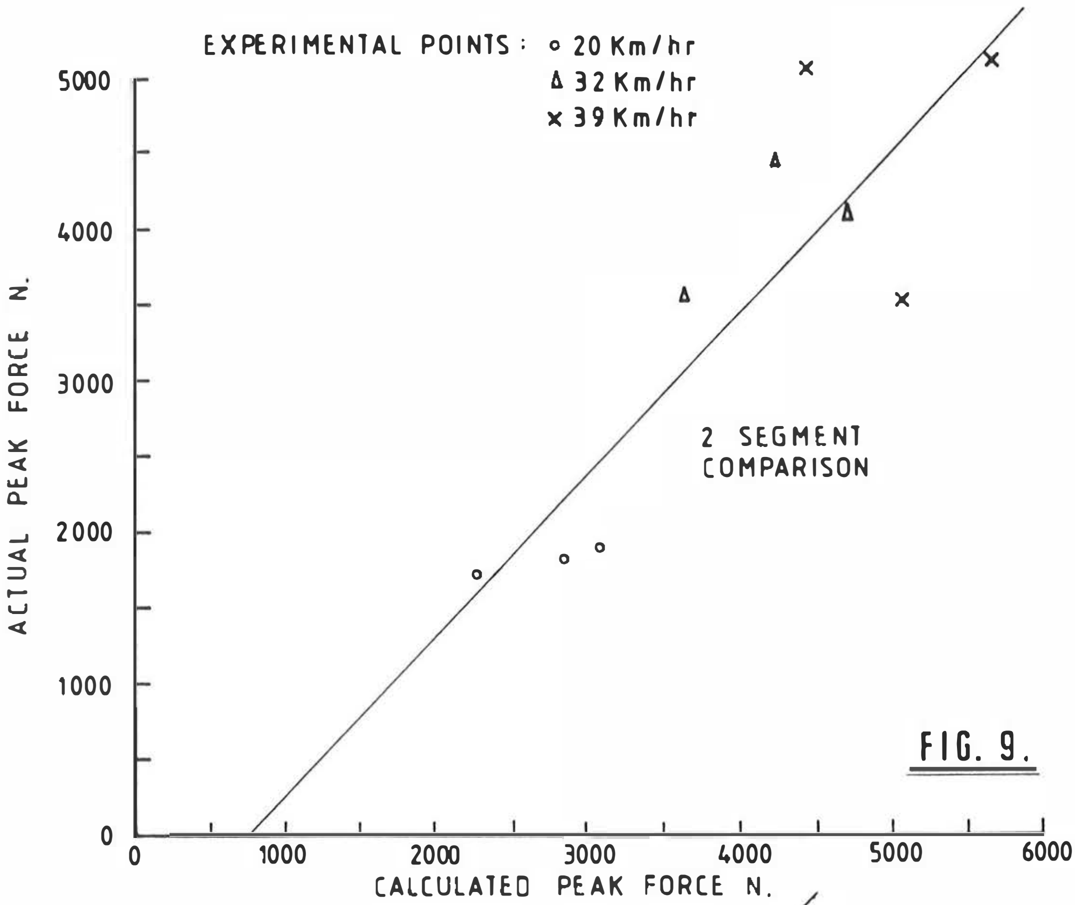

FIG. 9.

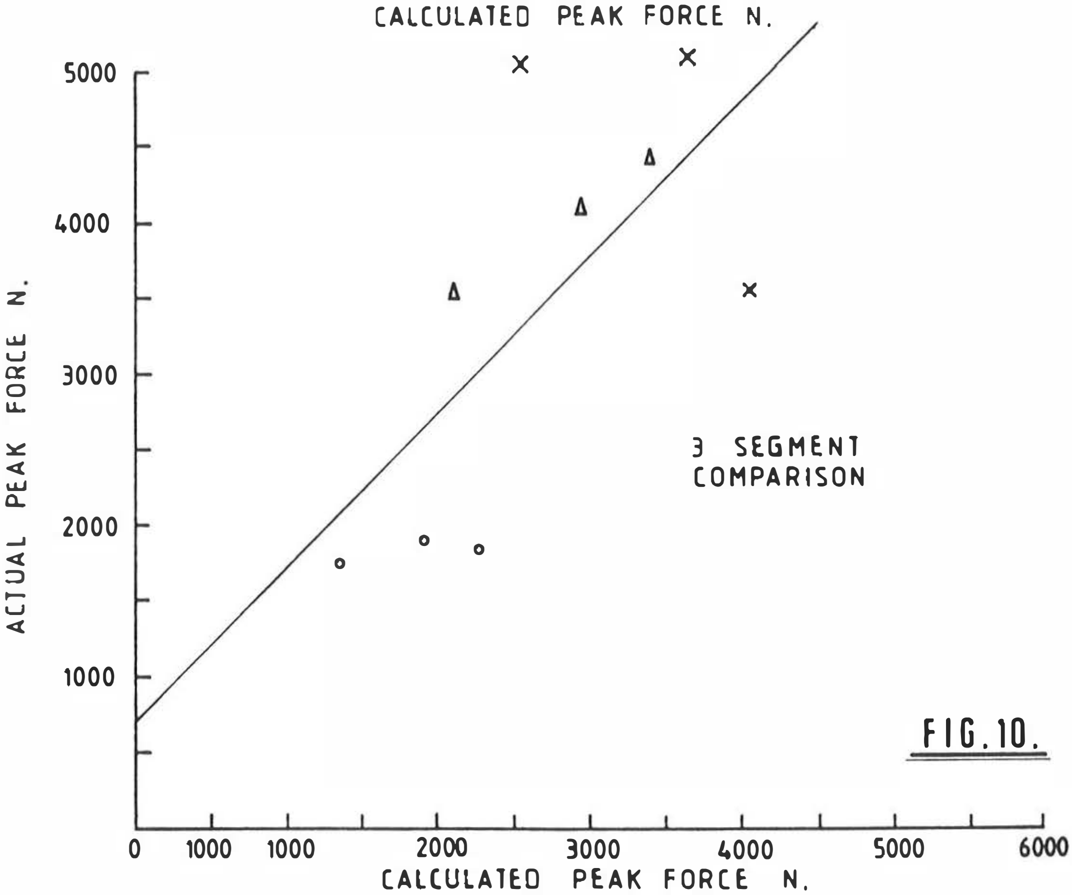

FIG.10.

PEAK IMPACT FORCE on LEG